

One- and two-phonon γ -vibrational bands in neutron-rich ^{107}Mo

J. Marcellino,^{1,2} E. H. Wang,^{1,*} C. J. Zachary,¹ J. H. Hamilton,¹ A. V. Ramayya,¹ G. H. Bhat,^{3,4,5} J. A. Sheikh,^{4,5} A. C. Dai,⁶ W. Y. Liang,⁶ F. R. Xu,⁶ J. K. Hwang,¹ N. T. Brewer,^{1,†} Y. X. Luo,^{1,7} J. O. Rasmussen,⁷ S. J. Zhu,⁸ G. M. Ter-Akopian,⁹ and Yu. Ts. Oganessian⁹

¹Department of Physics and Astronomy, Vanderbilt University, Nashville, Tennessee 37235, USA

²Department of Physics, Union University, Jackson, Tennessee 38305, USA

³Department of Physics, Government Degree College Kulgam, Kulgam, Jammu and Kashmir 192 231, India

⁴Cluster University Srinagar, Srinagar, Jammu and Kashmir 190 001, India

⁵Department of Physics, University of Kashmir, Srinagar, Jammu and Kashmir 190 006, India

⁶School of Physics, Peking University, Beijing 100871, People's Republic of China

⁷Lawrence Berkeley National Laboratory, Berkeley, California 94720, USA

⁸Department of Physics, Tsinghua University, Beijing 100084, People's Republic of China

⁹Joint Institute for Nuclear Research, RU-141980 Dubna, Russian Federation

(Received 14 July 2017; revised manuscript received 9 August 2017; published 20 September 2017)

Neutron-rich ^{107}Mo has been reinvestigated by analyzing the large statistics γ - γ - γ and γ - γ - γ - γ coincidence data from the spontaneous fission of ^{252}Cf at the Gammasphere detector array. Two new bands have been identified. The potential-energy surface calculations of this nucleus have been performed. The calculations show evidence for the $5/2^+$ [413] configuration of the ground-state band and $7/2^-$ [523] configuration for the 348-keV excited band, as assigned in previous work. The two bands newly established are proposed to be one- and two-phonon γ -vibrational bands built on the $7/2^-$ [523] Nilsson orbital, respectively, in the current paper. Triaxial projected shell-model (TPSM) calculations have been performed to explain the level structure and are found in fair agreement with experimental data. In particular, the TPSM study confirms the γ - and $\gamma\gamma$ -vibrational structure for the two observed excited band structures. Systematics of the one- and two-phonon γ -vibrational bands in the $A \sim 100$ Mo series is also discussed.

DOI: [10.1103/PhysRevC.96.034319](https://doi.org/10.1103/PhysRevC.96.034319)

I. INTRODUCTION

In deformed nuclear structure, γ vibrations are a typical collective motion. The multiphonon γ -vibrational bands are one of the important aspects in deformed nuclei. The one- and two-phonon γ -vibrational bands in the $A \sim 100$ region were reported in many even-even nuclei, e.g., $^{102,104,106,108}\text{Mo}$ [1–7], $^{108,110,112,114}\text{Ru}$ [8–11], and ^{114}Pd [12]. However, few such multiphonon γ -vibrational bands have been observed for odd- A nuclei. These bands were identified in odd- A $^{103,105}\text{Mo}$ [13,14], and then in odd- A $^{103,105}\text{Nb}$ [15,16] and $^{107,109}\text{Tc}$ [17,18]. Moreover, recent theoretical calculations support three-phonon γ -vibrational bands in $^{103,105}\text{Nb}$ [19]. The ^{107}Mo nucleus lies between even-even $^{106,108}\text{Mo}$ with one- and two-phonon γ -vibrational bands reported for both the nuclei. Thus, it is likely that ^{107}Mo would have such bands.

In the previous study, the high spin states and energy levels of ^{107}Mo have been established via ^{248}Cm [20–22] and ^{252}Cf [23,24] spontaneous fission (SF) experiments and $^{238}\text{U}(\alpha, f\gamma)$ reaction [3]. The ground state of ^{107}Mo was tentatively assigned as $5/2^+$ [413] [20,21]. Two excited bands based on 66- and 348-keV levels were also established from those reports. The γ - γ angular correlation measurements have been used to determine I^π , mixing ratios (δ), and g factors [20–22,24]. Triaxiality is also proposed in this nucleus. However, no

γ -vibrational bands have been reported in this nucleus. In the present paper, we reinvestigated the high spin states of ^{107}Mo with our large statistics ^{252}Cf spontaneous fission data. New transitions and levels observed in the current paper suggest the existence of 1γ and 2γ bands in ^{107}Mo . Potential-energy surface (PES) and triaxial projected shell-model (TPSM) calculations have been carried out and the results support the configuration assignment. Triaxial projected shell-model calculations well reproduced the levels of ^{107}Mo .

II. EXPERIMENTAL METHOD

The present experiment was done at the Lawrence Berkeley National Laboratory with the Gammasphere detector array. A $62\text{-}\mu\text{Ci}$ ^{252}Cf source was sandwiched between two iron foils of 10 mg/cm^2 , which were used to stop the fission fragments and eliminate the need for a Doppler correction. A 7.62-cm-diameter plastic (CH) ball surrounding the source was used to absorb β rays and conversion electrons, as well as to partially moderate and absorb fission neutrons. A total of 5.7×10^{11} γ - γ - γ and higher-fold γ events, and 1.9×10^{11} γ - γ - γ - γ and higher-fold γ coincident events, were recorded. These γ coincident data were analyzed by the RADWARE software package [25]. More details about the experimental setup can be found in Refs. [26,27].

III. EXPERIMENTAL RESULTS

The new level scheme of ^{107}Mo is shown in Fig. 1. The result contains four band structures. The relative intensities of

*ehong.wang@vanderbilt.edu

[†]Present address: Physics Division, Oak Ridge National Laboratory, Oak Ridge, TN 37831, USA.

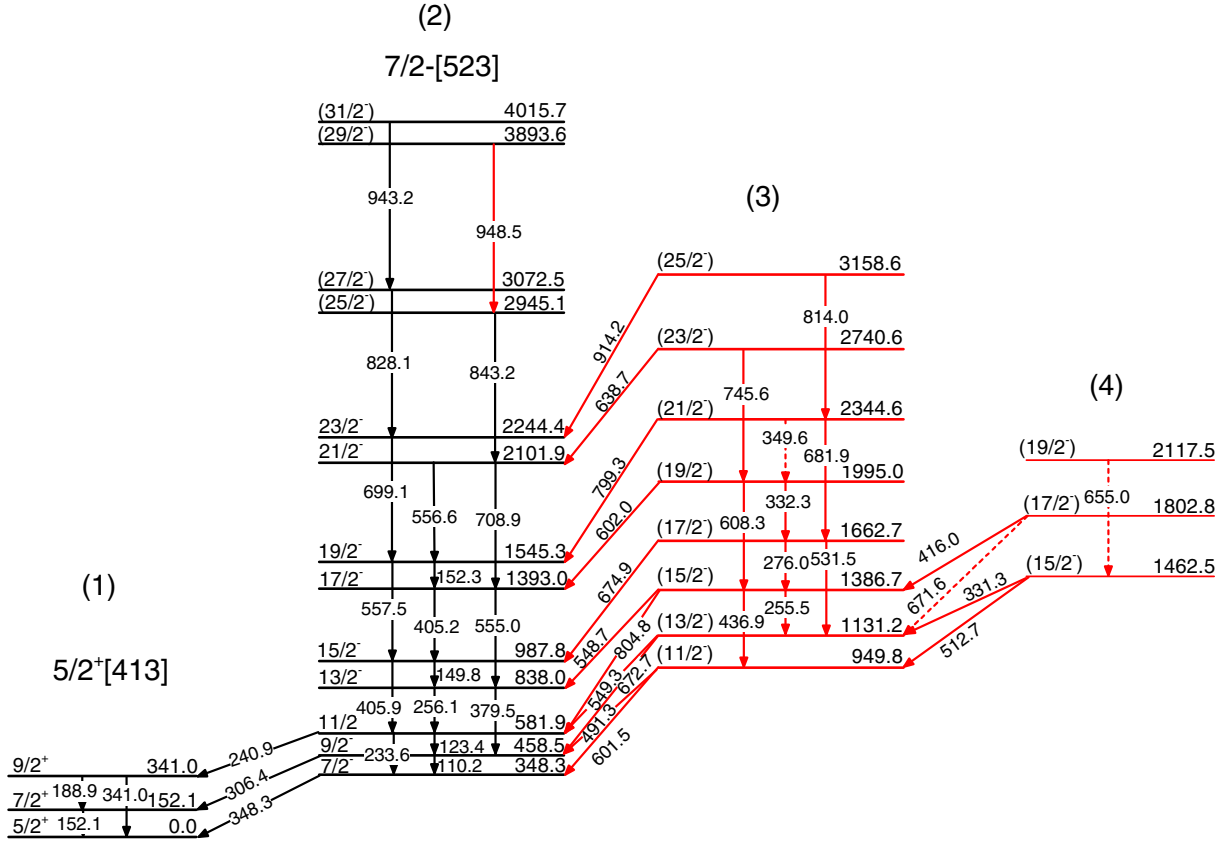


FIG. 1. The new level scheme of ^{107}Mo obtained in the present paper. The four bands are labeled 1–4. Band 1 is the ground-state band. The 948.5-keV transition in band 2 and all the transitions in bands 3 and 4 are newly identified. These new transitions are labeled in red (online). Note that only part of the ground-state band is shown.

the γ transitions and their energies are listed in Table I. The values have been normalized to the 348.3-keV transition that feeds the ground state. The ground-state band 1 and the $7/2^-$

band 2 were identified previously in ^{248}Cm [20–22] SF, ^{252}Cf SF [23,24], and $^{238}\text{U}(\alpha, F\gamma)$ reaction [3]. Note that only the first two excited levels in band 1 are drawn in the present paper. In

TABLE I. The relative intensities (I_γ) of the γ -ray transitions in ^{107}Mo , where E_i is the initial level energy and E_γ is the γ -ray energy. Here only the transitions in the current level scheme are listed.

E_γ (keV)	I_γ (%)	E_i (keV)	E_γ (keV)	I_γ (%)	E_i (keV)	E_γ (keV)	I_γ (%)	E_i (keV)
110.2	39(2)	458.5	379.5	20(1)	838.0	655.0	<0.5	2117.5
123.4	46(2)	581.9	405.2	4.1(4)	1393.0	671.6	<0.3	1802.8
149.8	10(1)	987.8	405.9	44(3)	987.8	672.7	3.4(4)	1131.2
152.1	94(5)	152.1	416.0	1.0(2)	1802.8	674.9	2.9(4)	1662.7
152.3	0.54(1)	1545.3	436.9	4.2(2)	1386.7	681.9	2.1(3)	2344.6
188.9	7.9(4)	341.0	491.3	3.9(2)	949.8	699.1	6.7(6)	2244.4
233.6	22(1)	581.9	512.7	1.7(2)	1462.5	708.9	2.9(5)	2101.9
240.9	7.7(4)	581.9	531.5	4.5(7)	1662.7	745.6	1.0(1)	2740.6
255.5	2.3(5)	1386.7	548.7	4.4(5)	1386.7	799.3	0.42(6)	2344.6
256.1	26(1)	838.0	549.3	9.4(6)	1131.2	804.8	1.6(1)	1386.7
276.0	0.30(8)	1662.7	555.0	11(1)	1393.0	814.0	0.61(1)	3158.6
306.4	37(2)	458.5	556.6	1.1(1)	2101.9	828.1	1.0(1)	3072.5
331.3	0.69(13)	1462.5	557.5	23(2)	1545.3	843.2	0.50(9)	2945.1
332.3	1.7(3)	1995.0	601.5	8.5(6)	949.8	914.2	0.19(3)	3158.6
341.0	55(3)	341.0	602.0	0.4(1)	1995.0	943.2	0.18(2)	4015.7
348.3	100	348.3	608.3	2.3(5)	1995.0	948.5	0.06(1)	3893.6
349.6	<0.5	2344.6	638.7	~0.1	2740.6			

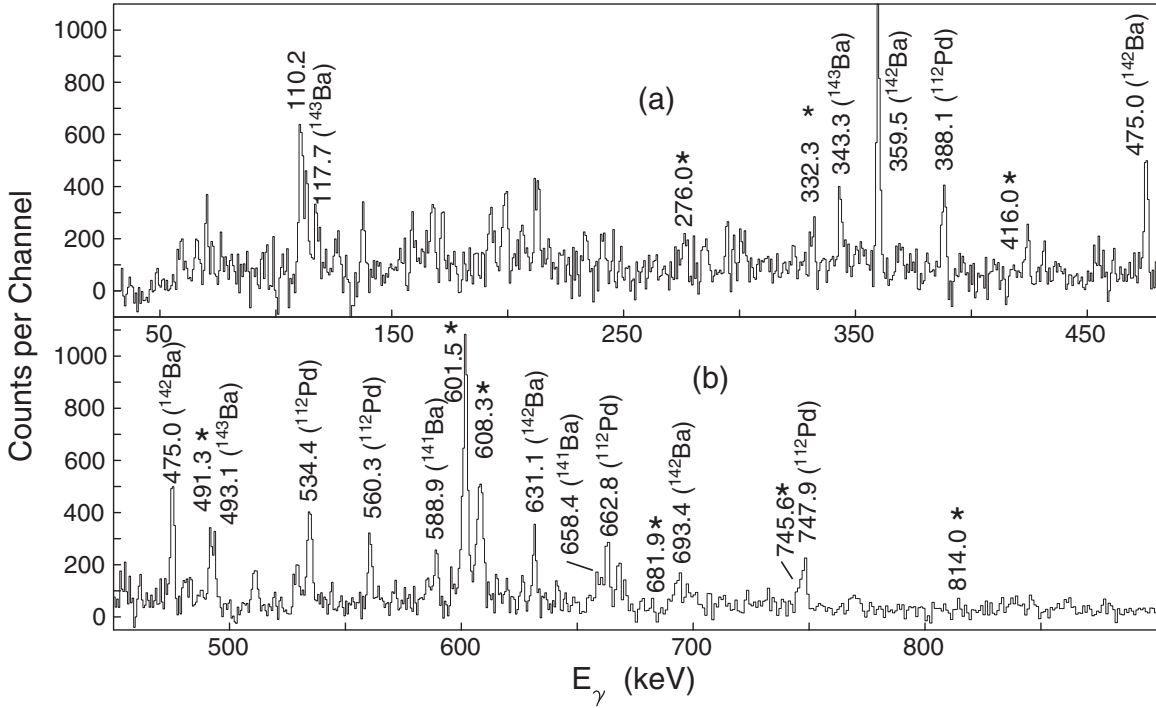


FIG. 2. Part (a) and (b) show the different energy regions of the partial γ -ray coincidence spectra by gating on 436.9- (new) and 348.3-keV transitions. New transitions are labeled with an asterisk.

Ref. [3], the negative parity $7/2^-$ band was established up to $35/2^-$. We have confirmed levels of this band (2) up to $31/2^-$ and added one more 948.5-keV transition ($29/2^-$) to this band.

Some γ -ray coincidence spectra are shown below. They are three examples of many coincidence spectra to cross-check and confirm the γ rays and level energies. The evidence of some strong new transitions is shown in Fig. 2. The coincidence spectra shown in Fig. 2 as well as the spectra in Figs. 3 and 4 are background subtracted. In Fig. 2, part (a) and (b) denote different energy regions of the 436.9-keV transition in band 3 and 348.3-keV transition in double gated spectra. This gate shows evidence for the transitions in band 3. The coincident 276.0-, 332.3-, (416.0)-, 491.3-, 601.5-, 608.3-, 681.9-, 745.6-, and 814.0-keV γ transitions can be seen. The $^{141,142,143}\text{Ba}$ fission partner transitions are also seen in the spectra. The 416.0-keV transition is not very clear in this double gate. More evidence will be shown later. The 388.1-, 534.4-, 560.3-, 682.2-, and 747.9-keV strong contamination transitions in ^{112}Pd come from the coincidence of the first $E2$ 348.8-keV transition in ^{112}Pd and the background.

Some of the weak transitions are not clearly seen in the gate with low-lying transitions, as shown in Fig. 2. However, they can be identified by gating on appropriate transitions at a higher level. Such evidence is shown in Figs. 3 and 4. Figure 3(a) denotes a partial γ -ray coincidence spectrum by double gating on the 348.3-, 123.4-, and 110.2-keV transitions. In this gate, the new transitions of 416.0-, 512.7-, 531.5-, 548.7-, 549.3-, and 608.3-keV transitions and the previously identified 149.8-, 152.3-, 256.1-, 405.2-, 555.0-, 556.6-, 557.5-, 699.1-, and 708.9-keV transitions in band 2 [3,20,23] can be seen. The fission partner transitions from $^{141,142,143}\text{Ba}$ are also seen. Part (b) of Fig. 3 depicts a double gated spectrum on the 549.3-

and 233.6-keV transitions. The 255.5-keV (M1) transitions in band 3 and 331.3-keV transition linking bands 3 and 4 can be seen. The 416.0-, 531.5-, and 608.3-keV transitions are also seen. In part (c) of Fig. 3, the partial γ -ray coincidence spectrum by gating on 557.5- and 405.9-keV transitions is shown. The new weak 416.0- and 608.3-keV transitions can be seen. The fission partner transitions from Ba are also seen. In Fig. 4, a γ -ray coincidence spectrum double gated on the 557.5- and 405.9-keV transitions in band 2 is shown. One can see the previously identified transitions in band 2 and the new linking transitions at 799.3 keV. The intensity of this transition is comparable with the 828.1-keV stretched $E2$ transitions in band 2.

IV. DISCUSSION

New PES calculations have been undertaken for the ^{107}Mo nucleus to address the configurations of the bands in ^{107}Mo . The configuration-constrained potential-energy surface method [28] is employed. The nonaxial deformed Woods-Saxon potential [29] with universal parameters has been used to generate single-particle levels. The Lipkin-Nogami method [30] is employed to avoid the spurious transition encountered in the BCS approach. The total energy of a nucleus can be decomposed into a macroscopic part obtained from the standard liquid-drop model and a microscopic part computed with the shell-correction approach including blocking effects. The deformation, excitation energy, and pairing property of a given state are determined by minimizing the obtained PES.

Table II shows PES calculated results of excitations and shape parameters for the quasiparticle states of configurations near the Fermi energy. From this table, the ground level is

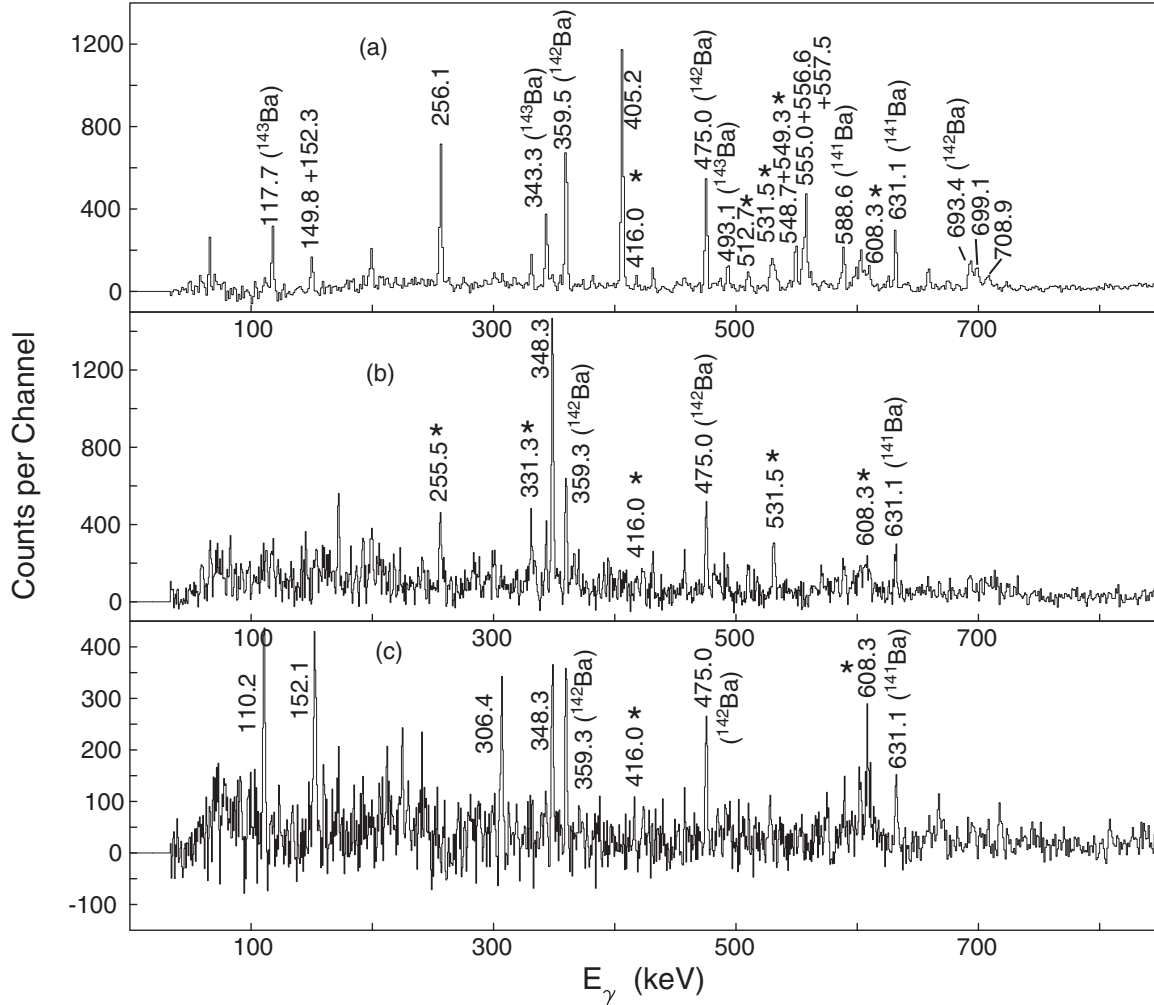


FIG. 3. Partial γ -ray coincidence spectrum by gating on (a) 348.3-, 123.4-, and 110.2-; (b) 549.3- and 233.6-; and (c) 548.7- and 379.5-keV transitions. New transitions are labeled with an asterisk.

assigned as $\nu 5/2^+[413]$ configuration, which has $\beta_2 = 0.331$, $\beta_4 = 0.002$, and $\gamma = -17^\circ$. This assignment is consistent with the quasiparticle-phonon coupling plus rotor model calculations in Ref. [21]. For the excited band 2 with a 348.3-keV bandhead, the angular correlation measurement in Ref. [20] confirmed $\Delta I = 1$ $E1$ for the 348.3-keV transition. Our calculation suggests a $\beta_2 = 0.328$, $\beta_4 = -0.003$, and $\gamma = -19^\circ$ triaxial deformation. Furthermore, the contour plot in Fig. 5 shows some softness of this configuration. The calculated excitation energy of this bandhead is also reasonably close to the experimental data.

The levels in new band 3 strongly decay to band 2 while the other new band 4 is only observed to decay to the new band 3. These two bands are not proposed to be single-particle bands, for the reason that the configurations listed in Table II have relative lower spins and are less likely to be populated in ^{252}Cf SF decay at such high energy. Furthermore, the proton and neutron pairing gaps at this region are about $2\Delta_p \sim 1.7$ MeV and $2\Delta_n \sim 2.1$ MeV, respectively [1]. Thus, the bands (3) and (4) with bandhead levels much less than those energies should not be three-quasiparticle bands. In

the present paper, the new bands (3) and (4) are assigned as one- and two-phonon γ -vibrational bands, respectively, and band 2 belongs to the zero-phonon γ -vibrational band. They originate from the $7/2^-[523]$ Nilsson orbital. Figure 6 shows systematical comparison of the levels of the 0γ -, 1γ -, and 2γ -vibrational bands in $^{103-108}\text{Mo}$ nuclei. Data are taken from Refs. [1–3,5–7,13] and the present paper. The level patterns of ^{107}Mo resemble the neighboring $A \sim 100$ Mo nuclei. The 0γ , 1γ , and 2γ bandhead energies and the $(E_{2\gamma} - E_{0\gamma})/(E_{1\gamma} - E_{0\gamma})$ ratios for some Nb, Mo, Tc, and Ru nuclei are compared in Table 3 of Ref. [13]. The harmonic value of this ratio should be 2, while the $(E_{2\gamma} - E_{0\gamma})/(E_{1\gamma} - E_{0\gamma})$ ratio in ^{107}Mo is somewhat smaller (1.85). For the odd- A Mo nuclei, the $(E_{2\gamma} - E_{0\gamma})/(E_{1\gamma} - E_{0\gamma})$ ratios increase from ^{103}Mo (1.55) [13] to ^{105}Mo (1.76) [7] to ^{107}Mo (1.85) (present paper), which shows a harmonic trend with increasing neutron numbers of the multiphonon γ -vibrational bands coupling to the $\nu h_{11/2}$ orbital. These values are all smaller than those in the even-even Mo nuclei, e.g., nearly harmonic 1.96 in ^{102}Mo , 1.95 in ^{104}Mo , 2.02 in ^{106}Mo , and large 2.43 in ^{108}Mo [13].

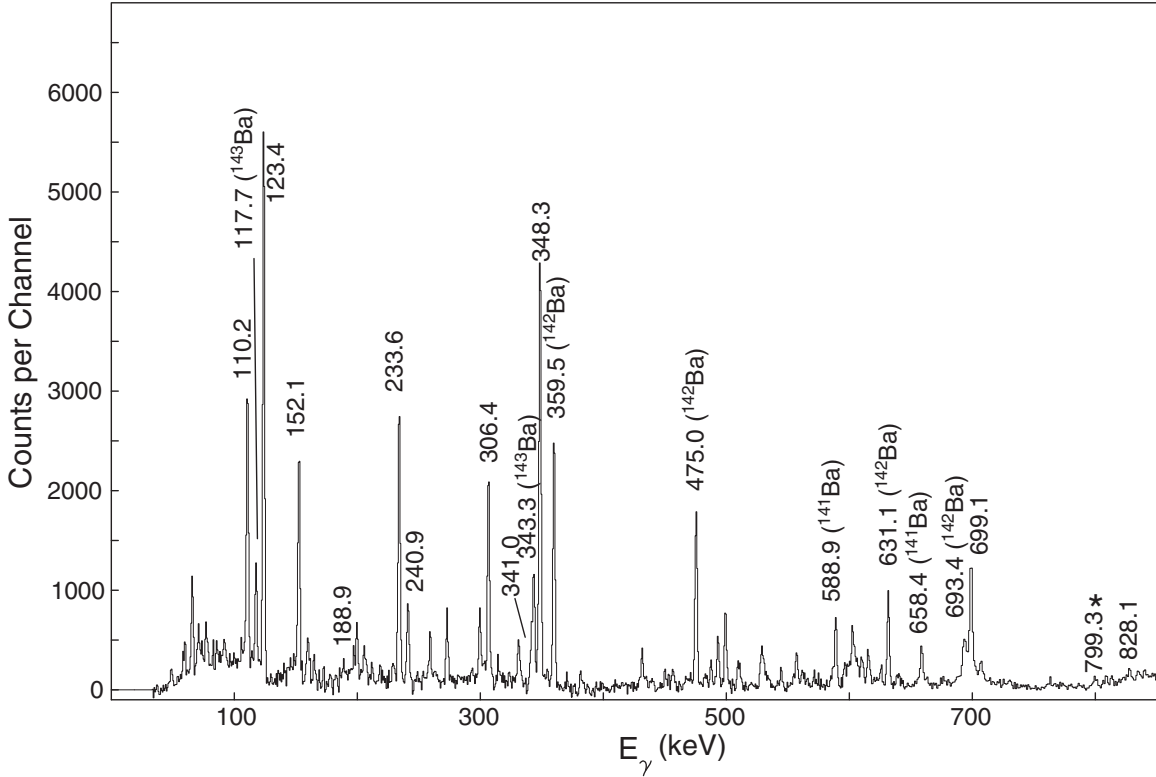


FIG. 4. Partial γ -ray coincidence spectrum by gating on 557.5- and 405.9-keV transitions. New transitions are labeled with an asterisk.

V. TRIAXIAL PROJECTED SHELL MODEL

It has been demonstrated [31] that the TPSM approach provides a unified description of the single-particle, vibrational, and rotational degrees of freedom. This model employs the deformed triaxial Nilsson wave functions as the basis states, which are the optimum basis to study deformed nuclei. The deformed bases are generated with the expected deformation of the nucleus under investigation. In this way, it is required to choose only a subset of the basis configurations that are close to the Fermi surface [32,33]. The axial deformation value is adopted from the measured quadrupole deformation, if available, otherwise from other theoretical approaches. The nonaxial deformation is chosen in such a manner that the bandhead energy of the γ band is reproduced.

TABLE II. Excited quasiparticle states of ^{107}Mo from PES calculation. Configurations, shape parameters, and excitation energies are indicated in the table.

Configuration	β_2	γ (deg)	β_4	E_{exc} (keV)
$v5/2^+[413]$	0.331	-17	0.002	0
$v5/2^-[532]$	0.315	-19	-0.003	88
$v7/2^-[523]$	0.328	-19	-0.003	597
$v3/2^+[411]$	0.349	0	-0.002	684
$v9/2^-[514]$	0.306	-23	-0.006	2227

TPSM calculations have been performed to obtain the excitation energies of the levels in ^{107}Mo . For ^{107}Mo , triaxial

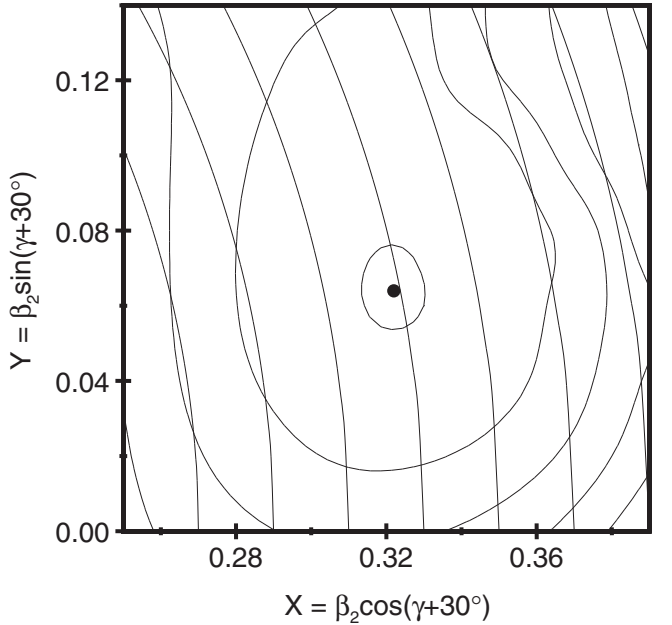


FIG. 5. A example of PES calculation for the $v7/2^-[523]$ configuration in ^{107}Mo at $\hbar\omega = 0$. The minimum is located at a deformation with $\beta_2 = 0.328$, $\gamma = -19^\circ$, $\beta_4 = -0.003$. The calculated excitation energy is $E_{\text{exc}} = 597$ keV relative to the $v5/2^+[413]$ ground state. The energy difference between each contour is 200 keV.

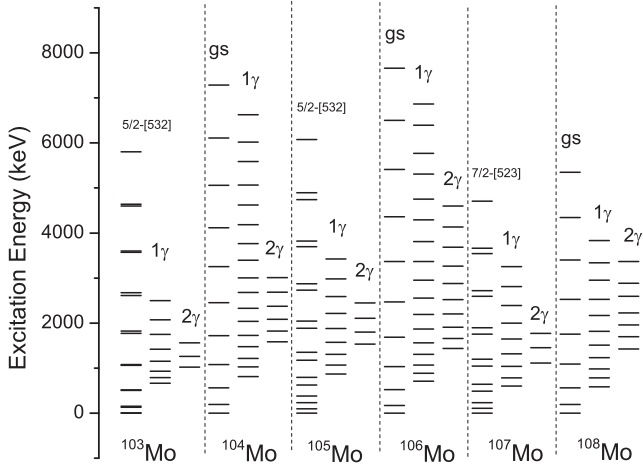


FIG. 6. Systematic comparisons of the 0γ -, 1γ -, and 2γ -vibrational bands in $^{103-108}\text{Mo}$.

bases have been obtained with the deformation values $\epsilon = 0.300$ and $\epsilon' = 0.17$ [31]. In the second stage, the deformed bases are projected onto states with good angular momentum by employing the three-dimensional angular momentum projection formalism [34–36]. The projected energies obtained from the quasiparticle configurations in the vicinity of the Fermi surface are displayed in Fig. 7. This figure, referred to as the band diagram, is quite useful in ascertaining the nature of the observed band structures. The lowest band structure corresponds to projected states from the $K = 7/2$ one-neutron quasiparticle state with energy -1.4743 MeV. The second lowest band is formed from the projection of the $K = 11/2$ one-neutron quasiparticle state with the same quasiparticle energy as that of the ground-state band. Therefore, this band structure is simply the γ band based on the $K = 7/2$ configuration. The third band structure results from the projection of the $K = 15/2$ configuration with the same quasiparticle energy as that of the $7/2^-$ configuration and, therefore, is the $\gamma\gamma$ band based on the $K = 7/2$ configuration.

In the final stage, the projected bases are used to diagonalize the shell-model Hamiltonian consisting of pairing plus

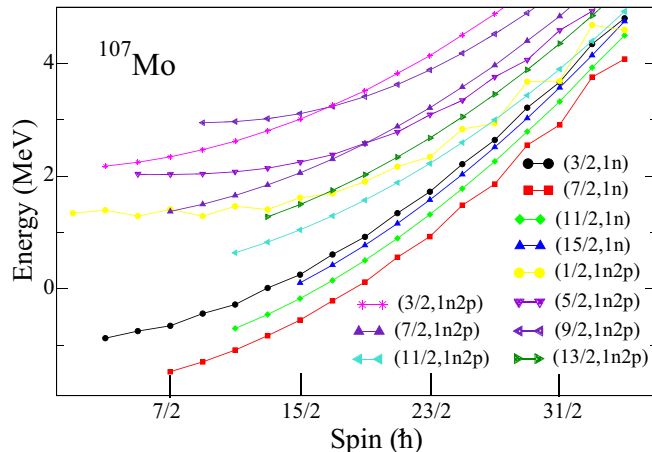


FIG. 7. The one- and three-quasiparticle band diagrams of ^{107}Mo .

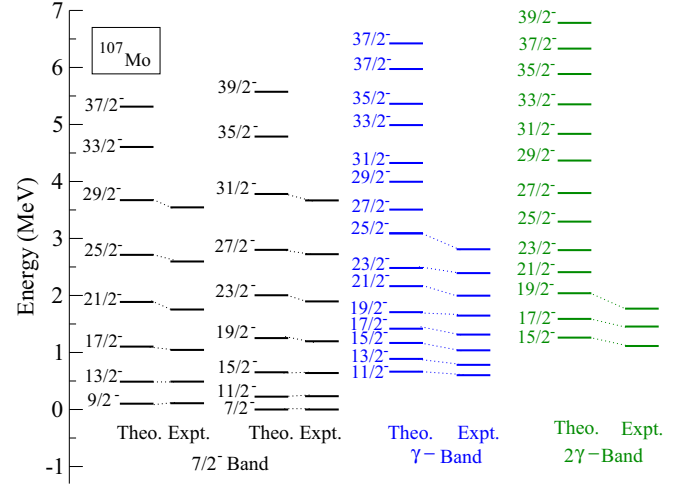


FIG. 8. Comparison of the TPSM calculation with experimental data. The level energies are normalized to the $7/2^-$ 0γ bandhead.

quadrupole-quadrupole interaction terms. TPSM calculated energies after diagonalization of the shell-model Hamiltonian are compared with the observed data in Fig. 8. It is evident from the figure that the TPSM approach reproduces the experimental data, in particular the $7/2^-$ band, quite well. Some deviations are noted for high spin states in the γ band and also for $\gamma\gamma$ bandhead energy. These differences have also been observed in our earlier studies [31,37,38] and are, primarily, due to the assumed fixed mean field (angular momentum projection after variation) in the TPSM calculations. In a more realistic treatment, projection ought to be performed before variation.

VI. CONCLUSION

In the present paper, a new high spin level scheme of ^{107}Mo has been established by analyzing the triple and fourfold γ -ray coincidence data from ^{252}Cf with Gammasphere. The two new observed bands are very similar to the one- and two-phonon γ -vibrational bands in neighboring Mo isotopes, respectively. We propose the bands to be such multiphonon γ -vibrational bands in ^{107}Mo . The PES calculation was used to interpret the shape of the ground-state band and the 348.3-keV excited band. TPSM calculation has been performed and is found to be in good agreement with the energy levels of the observed band structures in ^{107}Mo .

ACKNOWLEDGMENTS

The work at Vanderbilt University and Lawrence Berkeley National Laboratory was supported by the US Department of Energy under Grant No. DE-FG05-88ER40407 and Contract No. DE-AC03-76SF00098. The work at Tsinghua University was supported by the National Natural Science Foundation of China under Grant No. 11175095. The author would like to give special thanks for private communication with Yanxin Liu at Huzhou University.

- [1] A. Guessous, N. Schulz, W. R. Phillips, I. Ahmad, M. Bentaleb, J. L. Durell, M. A. Jones, M. Leddy, E. Lubkiewicz, L. R. Morss *et al.*, *Phys. Rev. Lett.* **75**, 2280 (1995).
- [2] R. Q. Xu, S. J. Zhu, J. H. Hamilton, A. V. Ramayya, J. K. Hwang, X. Q. Zhang, K. Li, L. M. Yang, L. Y. Zhu, C. Y. Gan *et al.*, *Chin. Phys. Lett.* **19**, 180 (2002).
- [3] H. Hua, C. Y. Wu, D. Cline, A. B. Hayes, R. Teng, R. M. Clark, P. Fallon, A. Goergen, A. O. Macchiavelli, and K. Vetter, *Phys. Rev. C* **69**, 014317 (2004).
- [4] Y. Y. Yang, S. J. Zhu, J. H. Hamilton, A. V. Ramayya, J. K. Hwang, J. O. Rasmussen, Y. X. Luo, K. Li, H. B. Ding, and J. G. Wang, *Chin. Phys. C* **33**, 199 (2009).
- [5] A. Guessous, N. Schulz, M. Bentaleb, E. Lubkiewicz, J. L. Durell, C. J. Pearson, W. R. Phillips, J. A. Shannon, W. Urban, B. J. Varley *et al.*, *Phys. Rev. C* **53**, 1191 (1996).
- [6] L. M. Yang, S. J. Zhu, K. Li, J. H. Hamilton, A. V. Ramayya, J. K. Hwang, X. Q. Zhang, L. Y. Zhu, C. Y. Gan, and M. Sakhaei, *Chin. Phys. Lett.* **18**, 24 (2001).
- [7] H. B. Ding, S. J. Zhu, J. H. Hamilton, A. V. Ramayya, J. K. Hwang, Y. X. Luo, J. O. Rasmussen, I. Y. Lee, X. L. Che, and J. G. Wang, *Chin. Phys. Lett.* **24**, 1021 (2007).
- [8] X. L. Che, S. J. Zhu, J. H. Hamilton, A. V. Ramayya, J. K. Hwang, J. O. Rasmussen, Y. X. Luo, Y. J. Chen, M. L. Li, and H. B. Ding, *Chin. Phys. Lett.* **21**, 1904 (2004).
- [9] S. J. Zhu, Y. X. Luo, J. H. Hamilton, A. V. Ramayya, X. L. Che, Z. Jiang, J. K. Hwang, J. L. Wood, M. A. Stoyer, R. Donangelo *et al.*, *Int. J. Mod. Phys. E* **18**, 1717 (2009).
- [10] X. L. Che, S. J. Zhu, J. H. Hamilton, A. V. Ramayya, J. K. Hwang, J. O. Rasmussen, Y. X. Luo, Y. J. Chen, M. L. Li, H. B. Ding *et al.*, *Chin. Phys. Lett.* **23**, 328 (2006).
- [11] E. Y. Yeoh, S. J. Zhu, J. H. Hamilton, K. Li, A. V. Ramayya, Y. X. Liu, J. K. Hwang, S. H. Liu, J. G. Wang, Y. Sun *et al.*, *Phys. Rev. C* **83**, 054317 (2011).
- [12] Y. Huang, S. J. Zhu, J. H. Hamilton, A. V. Ramayya, E. H. Wang, Y. X. Liu, Y. Sun, J. K. Hwang, Z. G. Xiao, H. J. Li *et al.*, *Int. J. Mod. Phys. E* **25**, 1650064 (2016).
- [13] H. Fryman-Sinkhorn, E. H. Wang, C. J. Zachary, J. H. Hamilton, A. V. Ramayya, G. H. Bhat, J. A. Sheikh, R. N. Ali, A. A. Wani, A. C. Dai *et al.*, *Int. J. Mod. Phys. E* **26**, 1750030 (2017).
- [14] H. B. Ding, S. J. Zhu, J. H. Hamilton, A. V. Ramayya, J. K. Hwang, K. Li, Y. X. Luo, J. O. Rasmussen, I. Y. Lee, C. T. Goodin *et al.*, *Phys. Rev. C* **74**, 054301 (2006).
- [15] J. G. Wang, S. J. Zhu, J. H. Hamilton, A. V. Ramayya, J. K. Hwang, S. H. Liu, K. Li, Y. X. Luo, J. O. Rasmussen, I. Y. Lee *et al.*, *Phys. Lett. B* **675**, 420 (2009).
- [16] H. J. Li, S. J. Zhu, J. H. Hamilton, A. V. Ramayya, J. K. Hwang, Y. X. Liu, Y. Sun, Z. G. Xiao, E. H. Wang, J. M. Eldridge *et al.*, *Phys. Rev. C* **88**, 054311 (2013).
- [17] L. Gu, S. J. Zhu, J. H. Hamilton, A. V. Ramayya, J. K. Hwang, S. H. Liu, J. G. Wang, Y. X. Luo, J. O. Rasmussen, I. Y. Lee *et al.*, *Chin. Phys. Lett.* **26**, 092502 (2009).
- [18] L. Gu, S. J. Zhu, J. H. Hamilton, A. V. Ramayya, J. K. Hwang, S. H. Liu, J. G. Wang, Y. X. Luo, J. O. Rasmussen, I. Y. Lee *et al.*, *Chin. Phys. Lett.* **27**, 062501 (2010).
- [19] M. Matsuzaki, *Phys. Rev. C* **90**, 044313 (2014).
- [20] W. Urban, T. Rząca-Urban, J. A. Pinston, J. L. Durell, W. R. Phillips, A. G. Smith, B. J. Varley, I. Ahmad, and N. Schulz, *Phys. Rev. C* **72**, 027302 (2005).
- [21] J. A. Pinston, W. Urban, Ch. Droste, T. Rząca-Urban, J. Genevey, G. Simpson, J. L. Durell, A. G. Smith, B. J. Varley, and I. Ahmad, *Phys. Rev. C* **74**, 064304 (2006).
- [22] A. G. Smith, J. L. Durell, W. R. Phillips, W. Urban, P. Sarriuguren, and I. Ahmad, *Phys. Rev. C* **86**, 014321 (2012).
- [23] J. K. Hwang, A. V. Ramayya, J. H. Hamilton, L. K. Peker, J. Kormicki, B. R. S. Babu, T. N. Ginter, C. J. Beyer, G. M. Ter-Akopian, and Yu. Ts. Oganessian, *J. Phys. G* **24**, 1013 (1998).
- [24] C. Goodin, A. V. Ramayya, J. H. Hamilton, N. J. Stone, A. V. Daniel, K. Li, S. H. Liu, J. K. Hwang, Y. X. Luo, J. O. Rasmussen *et al.*, *Phys. Rev. C* **80**, 014318 (2009).
- [25] D. C. Radford, *Nucl. Instrum. Methods Phys. Res., Sect. A* **361**, 297 (1995).
- [26] J. H. Hamilton, A. V. Ramayya, S. J. Zhu, G. M. Ter-Akopian, Yu. Ts. Oganessian, J. D. Cole, J. O. Rasmussen, and M. A. Stoyer, *Prog. Part. Nucl. Phys.* **35**, 635 (1995).
- [27] E. H. Wang, A. Lemasson, J. H. Hamilton, A. V. Ramayya, J. K. Hwang, J. M. Eldridge, A. Navin, M. Rejmund, S. Bhattacharyya, S. H. Liu *et al.*, *Phys. Rev. C* **92**, 034317 (2015).
- [28] F. R. Xu, P. M. Walker, J. A. Sheikh, and R. Wyss, *Phys. Lett. B* **435**, 257 (1998).
- [29] W. Nazarewicz, J. Dudek, R. Bengtsson, T. Bengtsson, and I. Ragnarsson, *Nucl. Phys. A* **435**, 397 (1985).
- [30] H. C. Pradhan, Y. Nogami, and J. Law, *Nucl. Phys. A* **201**, 357 (1973).
- [31] G. H. Bhat, J. A. Sheikh, Y. Sun, and R. Palit, *Nucl. Phys. A* **947**, 127 (2016).
- [32] K. Hara and Y. Sun, *Int. J. Mod. Phys. E* **4**, 637 (1995).
- [33] J. A. Sheikh and K. Hara, *Phys. Rev. Lett.* **82**, 3968 (1999).
- [34] P. Ring and P. Schuck, *The Nuclear Many Body Problem* (Springer-Verlag, New York, 1980).
- [35] K. Hara and S. Iwasaki, *Nucl. Phys. A* **332**, 61 (1979).
- [36] K. Hara and S. Iwasaki, *Nucl. Phys. A* **348**, 200 (1980).
- [37] J. A. Sheikh, G. H. Bhat, Y. X. Liu, F. Q. Chen, and Y. Sun, *Phys. Rev. C* **84**, 054314 (2011).
- [38] C. L. Zhang, G. H. Bhat, W. Nazarewicz, J. A. Sheikh, and Y. Shi, *Phys. Rev. C* **92**, 034307 (2015).